Exhaust gas recirculation cooler fouling morphology: Characterisation, spatiotemporal nature, and system variable-morphology-property correlation

Article *in* Powder Technology · February 2025

DOI: 10.1016/j.powtec.2025.120786

Yipeng Yao
University of Mons

Zinong Zuo
Xihua University

Marie-Eve Duprez
University of Mons

Exhaust Gas Recirculation Cooler Fouling Morphology: Characterisation, Spatiotemporal Nature, and System Variable-Morphology-Property Correlation

Yipeng Yao [1, 2, 3, *], Zhiqiang Han [2, 3, **], Liping Luo [2], Hai Du [2], Wei Tian [2], Xueshun Wu [2], Zinong Zuo [2], Marie-Eve Duprez [1], Guy De Weireld [1]

1. Thermodynamics and Mathematical Physics Unit, Faculty of Engineering, University of Mons, Place du Parc 20, Mons, 7000, Belgium
2. Key Laboratory of Fluid and Power Machinery, Ministry of Education, Xihua University, Chengdu 610039, China
3. Engineering Research Center of Ministry of Education for Intelligent Air-Ground Fusion Vehicles and Control, Xihua University, Chengdu 610039, China

* Corresponding author:
E-mail address: yipeng.yao@umons.ac.be (Yipeng Yao).

** Corresponding author:
E-mail address: hanzq@mail.xhu.edu.cn (Zhiqiang Han).

Abstract

Fouling is one of the primary causes of failure in exhaust gas recirculation (EGR) coolers. Morphology may provide a powerful perspective for understanding the mechanisms, behaviours, and properties of fouling. However, a systematic review of fouling morphology is currently lacking. Considering the substantial progress made in morphology-related studies within the industry in recent years, this work reviews the findings on EGR cooler fouling morphology from four aspects: characterisation (scale, object, category, and technique), spatiotemporal nature, variable-morphology correlation, and morphology-property correlation. Furthermore, the current challenges and opportunities in this field are discussed. Based on this, we propose a framework for the morphological characterisation of EGR cooler fouling. It is demonstrated that morphology plays a crucial role in revealing the spatiotemporal characteristics of fouling, the formation and removal mechanisms, and the correlations among system variables, morphology, and properties. Morphology still holds significant potential in four areas: multi-scale and quantitative characterisation, nomenclature and taxonomy, and full lifecycle evolution. The findings provide a morphological perspective for fouling research within the industry and contribute to advancing the science of fouling morphology.

Keywords: Morphology; Fouling; Characterisation; Spatiotemporal Nature; Exhaust Gas Recirculation Cooler.

1. Introduction

Exhaust gas recirculation (EGR) cooling technology has become a key approach for suppressing nitrogen oxide emissions from internal combustion engines due to its dilution, thermal, and chemical effects [1, 2]. However, particulate deposition and vapour condensation in exhaust gases form a complex mixture known as fouling [3, 4]; it is defined as the accumulation of unwanted deposits on surfaces [5]. Numerous studies have reported that fouling leads to reduced heat transfer efficiency and increased pressure drop [6, 7]; in severe cases, it may even result in complete blockage [8, 9]. Therefore, the issue of fouling warrants significant attention.

Researchers in the industry have conducted extensive and in-depth reviews of EGR cooler fouling. Hoard et al. [10] were the first to review the fundamental aspects of this topic, including the concept, characteristics, deposition, stabilisation, and recovery of fouling. Subsequently, Abd-Elhady et al. [11] expanded on this by addressing additional critical topics, such as the functions of EGR coolers, descriptions of fouling issues, their fundamental mechanisms, and the role of catalyst addition. Abarham et al. [12] and Han et al. [13] not only focused on the deposition mechanisms of fouling but also considered its removal mechanisms. Paz et al. [14] provided a specialised report on the numerical modelling of fouling processes, while Yao et al. [4] concentrated on reviewing the pathways of vapour condensation within coolers and its consequences on fouling. These reviews collectively demonstrate that past studies have systematically examined EGR cooler fouling from various perspectives, achieving substantial progress.

It has been observed that no retrospective studies on the morphology of EGR cooler fouling currently exist. However, morphology plays a crucial role in analysing fouling issues. At present, the industry commonly uses the thermal fouling resistance curve to describe the three stages of fouling growth: the initiation phase, the roughness-controlled phase, and the layer growth phase [15]. The advantage of this method is that it allows for a rough understanding of fouling growth inside heat exchangers through external monitoring of thermal resistance. However, this approach is based on the correlation between fouling and thermal resistance, providing only indirect evidence and failing to fully characterise the actual fouling growth process. Morphology can address this limitation by directly observing and unbiasedly recording the entire fouling growth process. For example, Løge et al. recently used high-resolution X-ray micro-computed tomography to visualise the process of crystal formation [16], revealing the complex process of multi-component mixed crystallisation, which cannot be achieved by the thermal fouling resistance curve. Beyond the growth process, morphology also provides valuable insights into other fouling evolution processes. For instance, Paz et al. observed colour changes during the ozone treatment of fouling to reflect the depth of the reaction between ozone and fouling [3]. In summary, morphology offers a direct and clear perspective for addressing fouling issues.

Given the importance of morphology and the current lack of systematic reviews on EGR cooler fouling morphology, this study aims to comprehensively review the progress in this field. The review covers four key aspects: morphological characterisation (object, scale, category, and method, with a particular emphasis on real-time in-situ characterisation), spatiotemporal distribution characteristics of morphology, variable-morphology correlations, and morphology-property correlations. Finally, the challenges and opportunities in this field are discussed. This work not only systematically summarises the key findings in this area but, more importantly, helps clarify the potential role of morphology in analysing fouling issues, providing valuable references for future research.

2. Methodology

This work follows the process illustrated in **Figure 1**, to discuss in detail four sub-topics of fouling morphology. This process is also divided into literature search, screening, and summarisation stages. The literature search section provides a detailed account of the search strings and literature libraries used. The screening phase aims to filter relevant publications. The summarisation phase synthesises key findings related to the four sub-topics, namely: the characterisation framework, spatiotemporal distribution characteristics, system variable-morphology correlations, and morphology-property correlations.

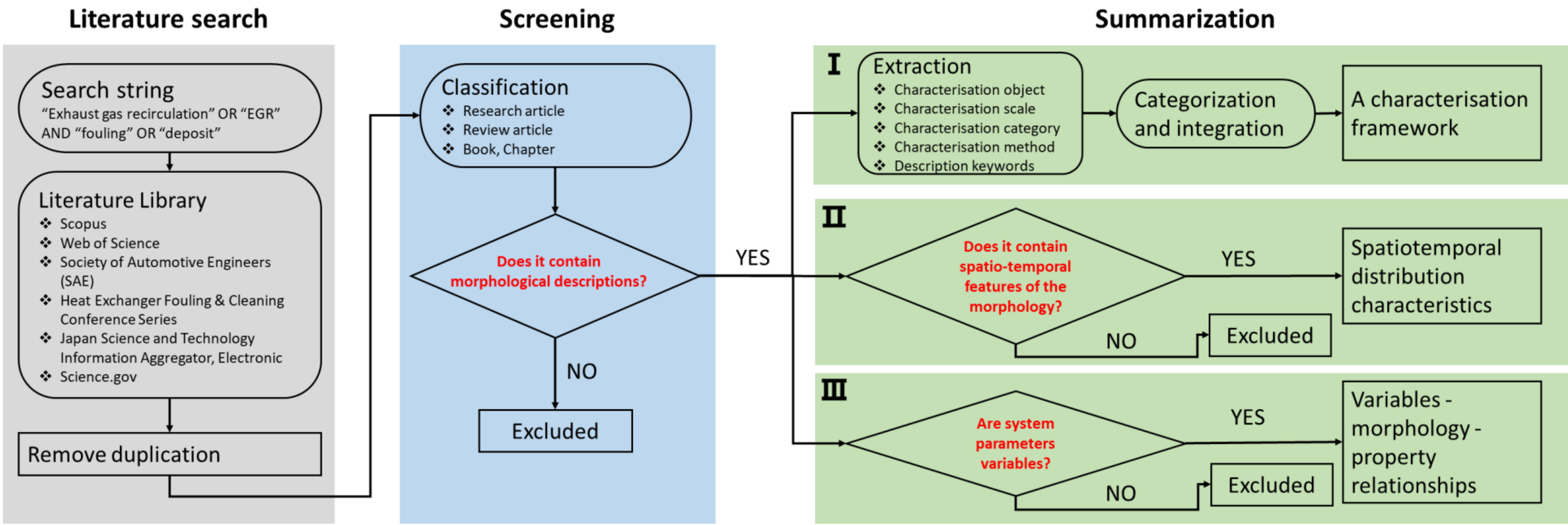

Figure 1. Flow of the overview for the EGR cooler fouling morphology

3. Characterisation of fouling morphology

3.1. A characterisation framework

The meta-information extracted following the process outlined in **Figure 1** is presented in **Table S1** of the supplementary document. Further refinement of this data has yielded a characterisation framework for EGR cooler fouling morphology, as illustrated in **Figure 2**. This framework encompasses four key components: characterisation scale, characterisation object, characterisation category, and characterisation method.

Regarding the characterisation scale, spanning from centimetre to nanometre levels, it can be further divided into four tiers: macroscopic, mesoscopic, microscopic, and nanoscopic. Correspondingly, the four levels of characterisation objects are distributed as follows: fouling layer, layering/cluster/large particulate, particulate matter, and primary particle. For each characterisation object, this work has distilled concise characterisation categories based on morphological descriptions from previous publications. Taking the fouling layer as an example, comprehensive characterisation can be conducted from eight categories: size, colour, shape, glossiness, wetness, compactness, roughness, and fragmentation. More importantly, this framework ultimately provides characterisation methods applicable to different scale levels and objects.

It is important to note that there is no strict correspondence between the four levels of characterisation objects and methods. This is because more advanced characterisation techniques often have downward compatibility. For instance, Scanning Electron Microscopy (SEM) can cover part of the working range of Optical Microscopy (OM), while Transmission Electron Microscopy (TEM) can, under certain conditions, partially replace SEM. Consequently, for the same characterisation category of a given object, multiple characterisation techniques may be available. For example, when the fouling volume is sufficient, qualitative observation of the fouling layer's roughness can be achieved through visual inspection or OM-based observation. This principle applies to other characterisation categories as well.

In summary, the proposed characterisation framework comprehensively addresses the aspects involved in EGR cooler fouling morphology characterisation, whilst, clearly delineating typical hierarchical levels. This framework serves as a valuable reference for future practitioners, reducing their exploratory time and enabling them to more effectively achieve their morphological characterisation objectives. Additionally, it facilitates more efficient intra-industry communication among practitioners, enhancing the accuracy of dialogue. Most crucially, this shared characterisation framework provides a solid foundation for further understanding the temporal evolution and spatial distribution patterns of fouling, as well as the correlations between variables, morphology, and properties.

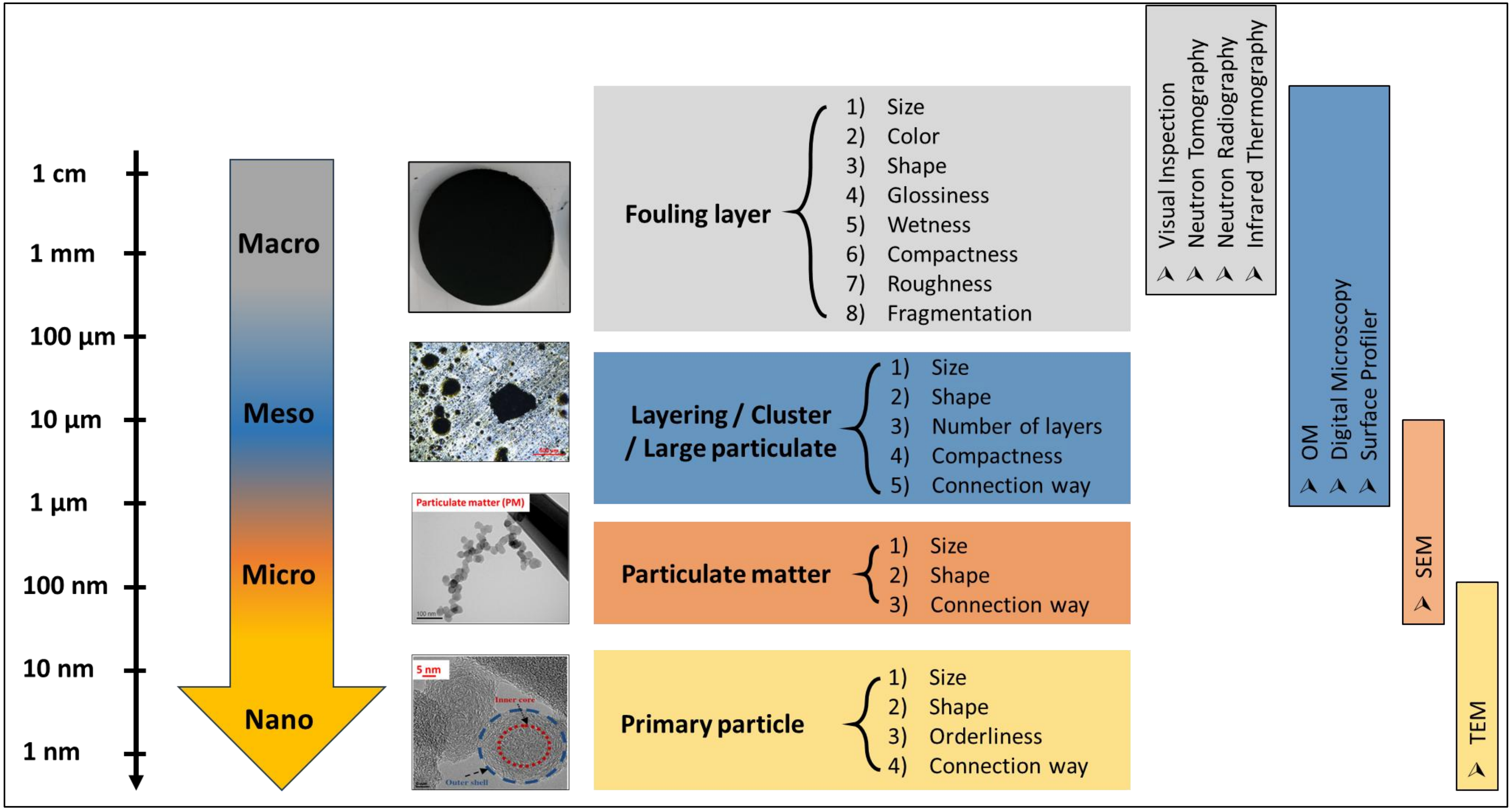

Figure 2. A characterisation framework (including characterisation scale, object, category, and technology) for the EGR cooler fouling morphology

3.2. In situ and real-time characterisation

Morphological characterisation is typically conducted by mechanically dissecting fouled coolers to expose the fouling, thereby facilitating the observation of its morphology, such as described in [17-19]. However, considering that environmental changes during the spatial relocation involved in sampling and preparing fouling specimens may damage their morphology and result in the loss of original features, in-situ characterisation has become a key topic of interest in the field. Similarly, fouling samples may undergo morphological evolution due to time-sequential events such as preparation, storage, and transportation following the fouling incident. As a result, real-time characterisation has also emerged as a prominent subtopic. Although in-situ and real-time characterisation focuses on spatial and temporal dimensions, respectively, real-time characterisation generally satisfies the requirements of in-situ characterisation as well.

The implementation of in-situ and real-time characterisation can be broadly divided into two strategies. The first involves using traditional experimental platforms combined with advanced optical techniques for characterisation. The second strategy upgrades experimental platforms to enhance accessibility while integrating characterisation technologies. For the first approach, Ismail et al. pioneered the development of the neutron radiography technique to perform in-situ, non-destructive measurements of fouling morphology, providing an accurate representation of fouling thickness and contours [20]. Similarly, Lance et al. employed neutron tomography to conduct in-situ tests of fouling morphology, achieving three-dimensional reconstructions of its structure [21]. For the second approach, Abarham et al. developed a visualised experimental platform combined with a digital microscope to record, in situ and in real-time, the morphological evolution of fouling during its formation or removal [22, 23]. Likewise, Salvi et al. utilised a visualised experimental platform along with optical and infrared testing techniques to achieve in-situ and real-time characterisation of the three-dimensional morphology of fouling [24].

4. The spatiotemporal distribution characteristics

4.1. Evolution of the fouling morphology

This section provides a comprehensive review of previous studies that have elucidated the generation, growth, and evolution processes of fouling in EGR coolers from a morphological perspective. It also examines how these studies contribute to our understanding of fouling mechanisms.

Firstly, morphological characterisation techniques effectively reveal the initial formation of fouling. Tanaka et al. observed protrusions on a stainless steel surface after 1 minute and 10 seconds, indicating the onset of fouling. The original images vividly illustrate the initial morphology of fouling formation. Furthermore, they monitored morphological changes over 16 minutes. Following the formation of hard fouling at 1 minute 10 seconds, particles continuously deposited and covered the hard fouling surface, creating a porous, powder-like deposit that continued to grow, eventually enveloping the underlying hard fouling completely [25]. This study meticulously documents the gradual growth process of fouling.

Li et al. provided detailed observations on how fouling growth progresses "from points to surfaces". Initially, particles with diameters of about tens of micrometres were scattered across the wall surface. As more particles are deposited, the size of these wall particles gradually increases. Individual particles began to be enveloped and started connecting with nearby particles. Eventually, after 1.5 hours, larger "dune-like" structures (approximately 50 μm or larger in length) were formed [26].

In addition to early-stage fouling observations, researchers have also investigated fouling morphology over longer time scales. Tanaka et al. used scanning electron microscopy to observe changes in fouling thickness over 24 hours period. They found that the thickness of both types of fouling increased linearly with time [25]. Li et al. compared fouling morphology at 22.5 hours and 31.5 hours. The authors noted that from around 22 hours into the experiment, the dune-like structures on the fouling surface began to disappear, and the surface morphology became smoother [26].

To quantify the degree of surface roughness in fouling, Li et al. introduced a parameter called the area ratio, defined as the ratio of the actual surface area to the corresponding projected area. They observed a decrease in the area ratio from 115% to 100% at 6.5 h, and 37 h, respectively, further corroborating the gradual smoothing of the surface morphology [26]. In a subsequent study by the same team, they employed a similar parameter, the SA ratio, defined as the ratio of the surface area of the deposit to the surface area of a comparable flat plate. Contrary to their earlier findings, they discovered that the SA ratio increased over time, possibly due to partial fouling agglomeration or the presence of large particles [27]. The introduction of these quantifiable parameters has undoubtedly enhanced the characterisation of fouling morphology, moving beyond mere qualitative descriptions.

Contradictory results regarding the temporal evolution of fouling morphology have also emerged in two other studies. Prabhakar and Boehman examined fouling morphology at different time intervals using low and high magnification, as shown in **Figure 3.** They observed that at 1.5 h, particles were randomly deposited on the tube surface. As time progressed, more particles accumulated on the existing layer, resulting in a completely covered and smooth, dense surface at 7.5 h [28]. In contrast, a recent quantitative study by Paz et al. measured surface roughness in three cases at 1.5 h, 3 h, 6 h, and 9 h. They found that roughness increased over time in all areas, particularly near the exhaust outlet, where roughness at 9 h was 2-3 times higher than at 6 h [29]. Broadly speaking, these findings suggest that fouling roughness can either decrease or increase over time, highlighting the complexity of this phenomenon.

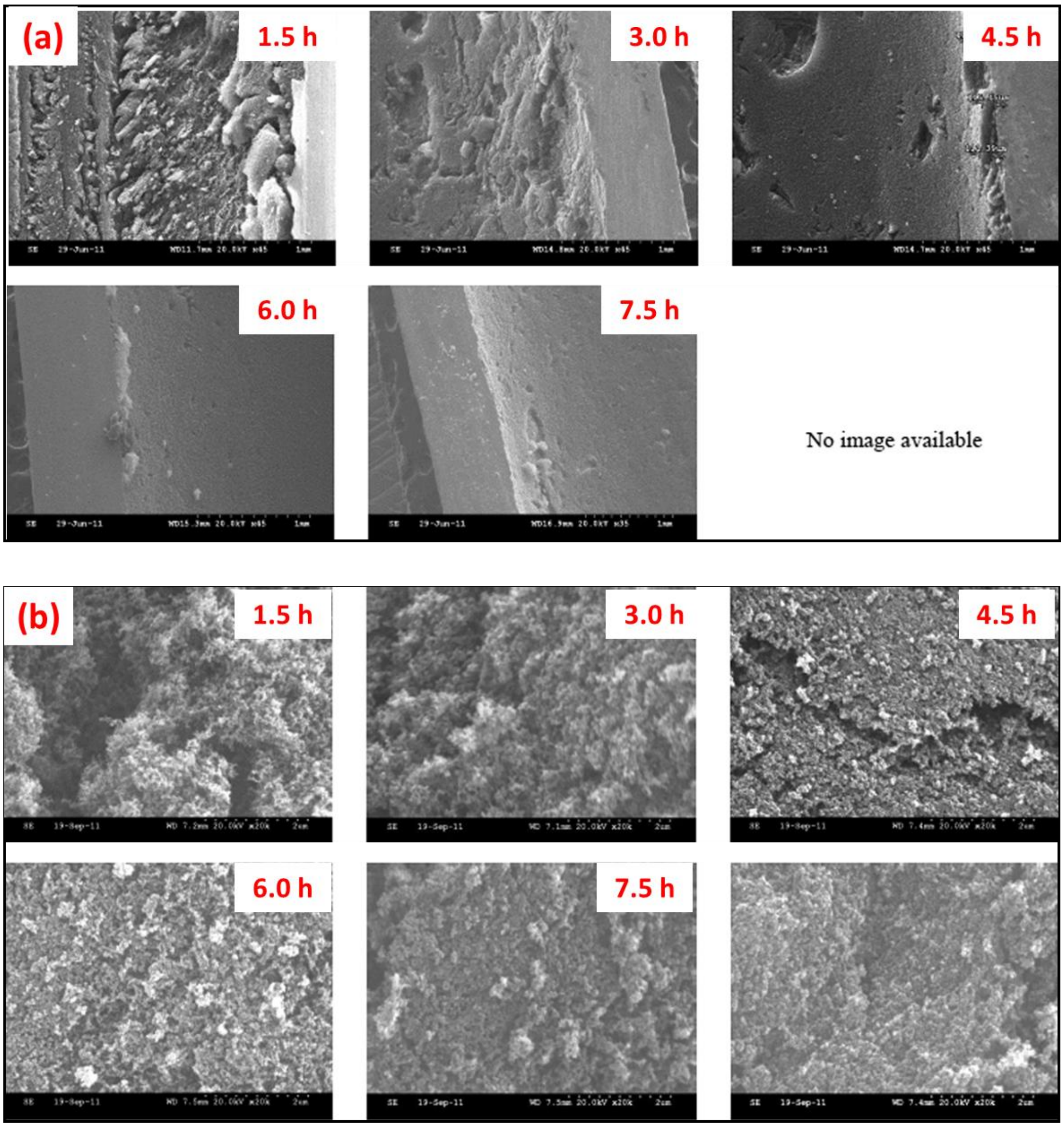

Figure 3. Variation of fouling microstructure as a function of time. (a) low magnification, (b) high magnification [28]

It is noteworthy that in the study by Prabhakar and Boehman, they established a correlation between morphological visual evidence and the heat exchange efficiency of coolers. They posited that once fouling completely covers the tube walls, the cooler's heat exchange efficiency begins to approach a certain value and remains stable [28]. This method of establishing connections further corroborates that, compared to indirectly reflecting fouling growth through parameters such as total thermal resistance or thermal efficiency, the morphological perspective not only provides a more intuitive approach but also offers a more fundamental interpretation for indirect methods.

In addition to the aforementioned morphological studies focusing on fouling formation and growth processes, several investigations have specifically examined the morphological changes during fouling removal [22, 23, 30]. For instance, in Furuhata et al.'s study, at 5 h, water vapour penetrated through the loose surface layer of fouling, condensing within the fouling layer. This caused the fouling to expand, elevating the surface layer, which subsequently detached under the influence of airflow. By 6 h, the expanded fouling had disappeared [30]. Similarly, Abarham et al. provided a more detailed account of the morphological changes during the formation of cracks before fouling removal and during the detachment process itself. As illustrated in **Figure 4**, these processes occur rapidly, typically completing crack growth and partial fouling detachment within 5 minutes. During this period, the morphology of the fouling is almost entirely transformed [22, 23].

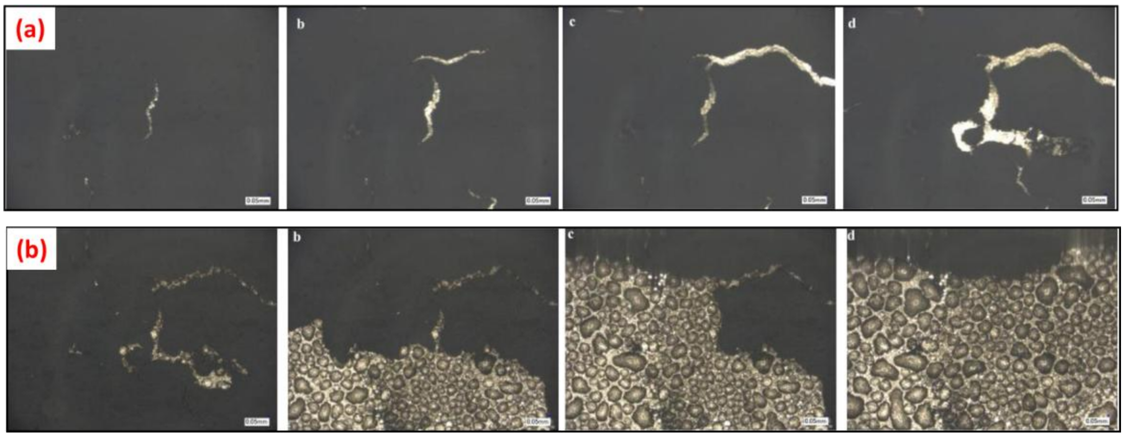

Figure 4. Cracks in fouling. Flow direction from left to right. (a) five-minute interval between successive images at 42°C, (b) one-minute interval between successive images at 20°C [23]

In conclusion, the morphology of fouling evolves over time, potentially becoming smoother or rougher, with surface undulations that may increase or decrease. Currently, there is no definitive consensus on these changes, necessitating further research to elucidate these controversies. However, there is agreement that when fouling is stripped away, the fragmentation of fouling rapidly increases. More significantly, the analysis of these results demonstrates that the characterisation of fouling morphology provides direct and compelling evidence for interpreting the processes of fouling generation, growth, removal, and stabilisation. This approach offers valuable insights into the complex dynamics of fouling phenomena.

4.2. Spatial distribution of fouling morphology

Spatial variations in fouling morphology manifest primarily in two aspects: microscopic differences across different layers in the cross-section and macroscopic differences along the direction of gas flow. The following sections provide a comprehensive summary of these morphological distribution characteristics in both dimensions.

The fouling cross-section consists of material between two characteristic interfaces: the gas-fouling interface and the fouling-tube interface. Styles et al. discovered that fouling can be divided into two layers: a highly dense hydrocarbon layer near the fouling-tube interface, and a particulate layer with a hydrocarbon distribution gradient further from this interface. This gradient is visually evident as a transition from dark near the gas-fouling interface to lighter near the fouling-tube interface [31]. Lance et al.'s research provided more intuitive evidence, revealing that the reflectivity of fouling is highest near the fouling-tube interface and gradually decreases towards the gas-fouling interface. This is due to variations in hydrocarbon condensation caused by thermal gradients within the fouling layer, with lower temperatures at the fouling-tube interface resulting in higher concentrations of condensed hydrocarbons. Consequently, fouling near the fouling-tube interface is more moist and dense, while fouling near the gas-fouling interface is drier and more porous [32]. Another study by Lance et al. found that fouling near the gas-fouling interface is significantly finer and less dense [17]. Tanaka et al.'s experimental results also confirmed this morphological difference, terming the fouling near the gas-fouling interface as a "powdery deposit" and that near the fouling-tube interface as a "lacquer deposit" or "hard deposit". Despite the nearly identical original composition of both layers, the former exhibits a highly porous structure, while the latter presents a dense structure [18].

The layered phenomenon of fouling has prompted researchers to observe its internal connecting structure through morphological methods. As shown in **Figure 5**, in addition to the significant density differences observed in the cross-section of fouling, it is evident that the dense and loose layers of fouling are typically connected by columnar structures [33]. Although different studies have varying nomenclature for the fouling layers, the findings consistently show that the top layer of fouling is supported on the bottom layer by multiple columnar structures [25, 32].

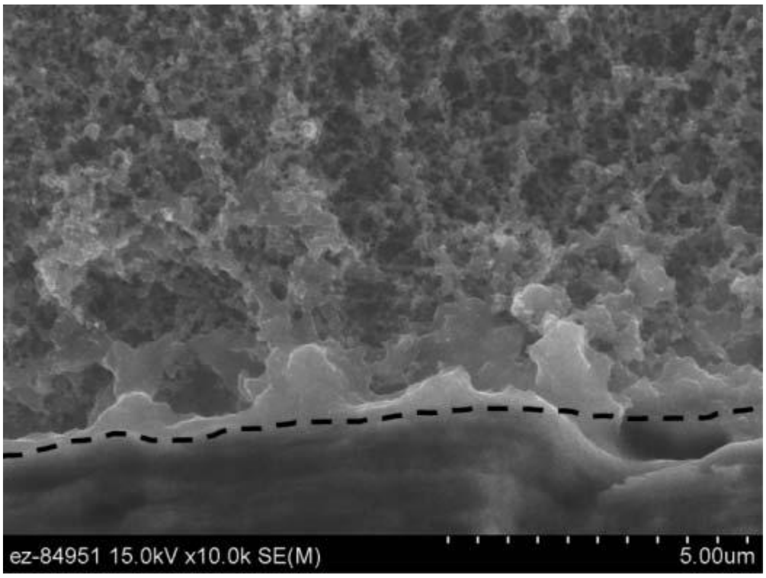

Figure 5. Fouling interlayer columnar connections [33].

It is worth noting that, unlike other areas, the morphology of fouling at the gas-fouling interface is particularly distinctive. **Figure 6** illustrates the fouling morphology at the gas side at 2,000x magnification, presenting a dendritic structure referred to as dendrites. These dendrites, approximately several tens of micrometres in height, are formed by the aggregation of particles and incline in the direction of waste gas flow [33]. These dendrites are highly porous internally, resembling fluffy cotton, and are dispersed at the gas-fouling interface [25, 34]. However, Storey et al. suggest that such morphologies are not observed on fouling layers with high hydrocarbon content [33].

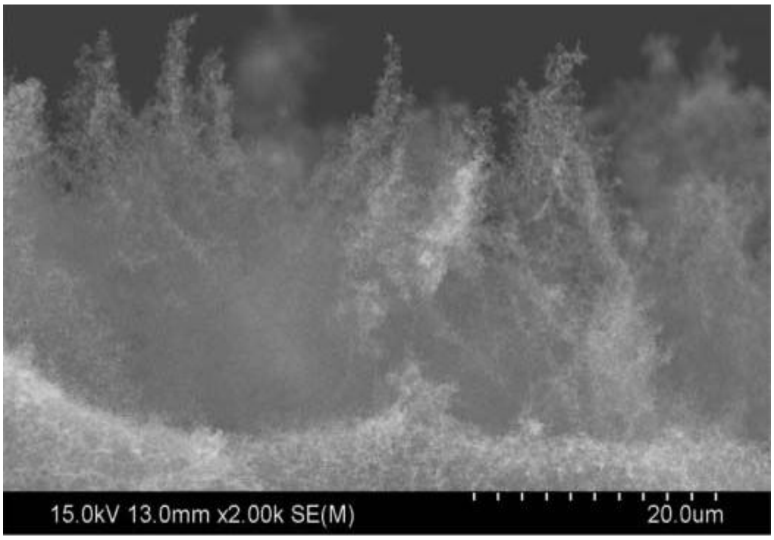

Figure 6. Dendritic form of fouling in the gas-fouling interface (2 KX) [33].

Based on the comparison of fouling cross-sectional morphologies, significant differences in glossiness, wetness, and compactness exist among different layers. This is because the temperature at the fouling-tube interface is lower than that at the gas-fouling interface, which is more conducive to hydrocarbon condensation. The condensed hydrocarbons, in turn, alter the morphology of the fouling. Interestingly, this research demonstrates how the differences in fouling morphology can be used to inversely deduce the degree of involvement of various fouling mechanisms, particularly reflecting the extent of hydrocarbon condensation within the fouling.

Along the gas flow direction, the overall morphology of fouling exhibits an increasing trend in roughness. As shown in **Figure 7 (a)**, Tian et al.'s experimental results demonstrate that from upstream to downstream of the cooler, the fouling morphology continuously changes, with downstream locations showing rougher fouling and more pronounced grooves [35]. In the same year, Al-Janabi and Malayeri observed that fouling at the inlet of a smooth plate was more uniform, while fouling in the middle and outlet areas was more uneven, with scratches and grooves appearing [36], as illustrated in **Figure 7 (b)**. Paz et al. employed more advanced testing methods to showcase three-dimensional surfaces of fouling at different cooler locations, as depicted in **Figure 7 (c)**. The results indicate that fouling at the inlet is very smooth, while the fouling surface at the outlet exhibits mud cracks. They attributed this morphological difference to structural changes in fouling caused by the condensation and evaporation of hydrocarbons [37]. In another study, they quantitatively compared the roughness of the same parts of the fins (the windward side of the fin foot) at the cooler inlet and outlet, finding that the roughness at the outlet was greater compared to the inlet [29].

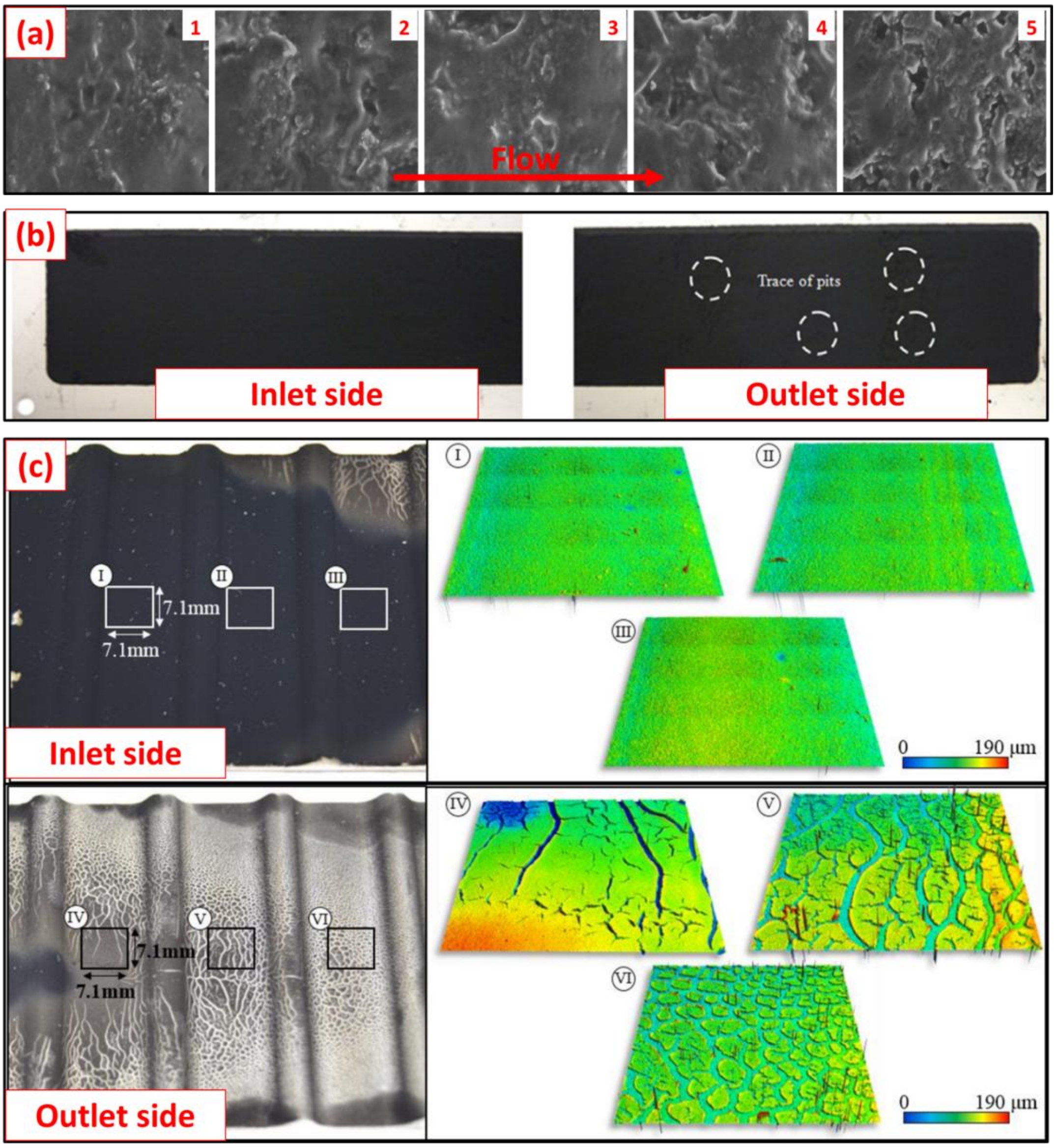

Figure 7. Fouling roughness distribution along the airflow direction. (a) Tian et al. [38], (b) Al-Janabi and Malayeri [36], (c) Paz et al. [37].

Fouling colour also changes along the gas flow direction. Han et al. observed that due to the continuous temperature decrease along the gas flow direction, the colour of the fouling gradually deviates from black at the outlet compared to the black fouling composed of dry carbon soot at the inlet. This is attributed to the intensified condensation of heavy hydrocarbons [39], as shown in **Figure 8 (a)**. Vence et al.'s experimental results corroborated this observation, as illustrated in **Figure 8 (b)**, where the chemical colouration and wet fraction of fouling increase along the gas flow direction. This phenomenon stems from the lower downstream temperatures, leading to increased hydrocarbon condensation and, consequently, colour variations [40].

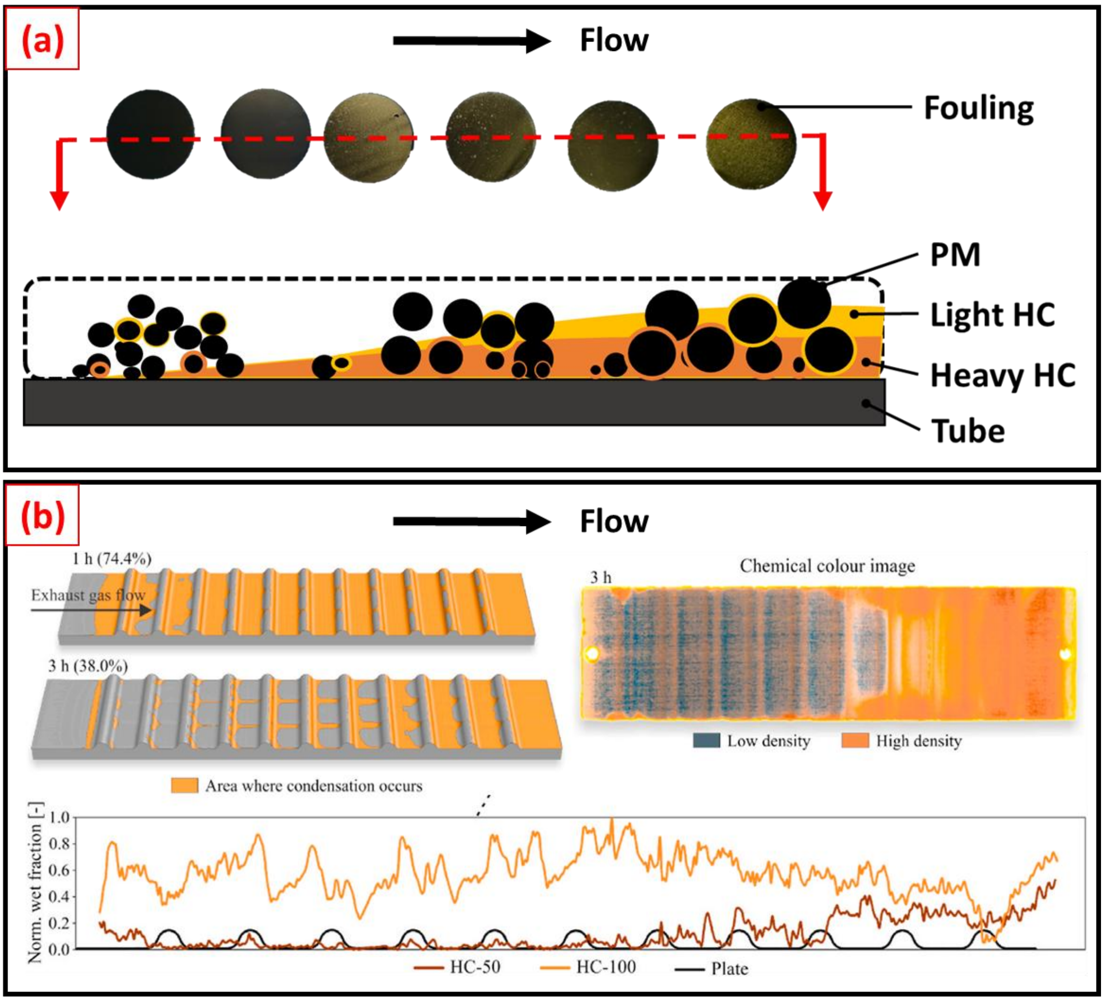

Figure 8. Fouling chemical colour distribution along the airflow direction. (a) Han et al. [39], (b) Vence et al. [40].

Beyond surface morphology differences along the gas flow direction, variations in cross-sectional morphological details have also been identified. Lance et al. confirmed that compared to the inlet, the middle section of fouling exhibits an increase in shiny layers, indicating more hydrocarbon condensation [17]. Paz et al.'s findings align with this, revealing that fouling at the outlet contains more oily substances compared to dry fouling at the inlet [37]. Yoo et al. compared the top layer morphology of fouling at the front, middle, and rear of the cooler. They discovered that dendrites grow larger and taller along the gas flow direction. This was attributed to the reduction in effective exhaust gas flow area as fouling accumulates, resulting in increased gas velocity and shear force at the gas-fouling interface. Consequently, dendrites at the interface tilt and break, developing into larger and taller structures [34]

Fouling morphology exhibits significant variations along the gas flow direction, specifically in terms of roughness, colour, glossiness, and dendrite size. These differences provide crucial evidence for interpreting fouling mechanisms: roughness changes may reflect the impact of large particle impingement and hydrocarbon condensation; colour and glossiness variations may indicate changes in hydrocarbon condensation intensity; dendrite size differences may reflect the interplay between removal and deposition mechanisms at the interface.

This section comprehensively reviews the temporal and spatial distribution characteristics of fouling morphology. From a temporal perspective, morphological changes effectively reflect the generation, growth, removal, and stabilisation behaviours of fouling. From a spatial perspective, morphology provides important evidence for decoding fouling deposition and removal mechanisms.

5. The system variable – morphology correlation

Table 1 provides a concise summary, in chronological order, of the 22 past studies identified in this work that investigated the correlation between system variables and fouling morphology. It can be observed that the system variables involved are quite extensive, including cooler structure, flow rate, engine operating conditions, coolant temperature, engine start-up mode, mass flow rate, baking temperature, fuel type, wall temperature, soot concentration, hydrocarbon concentration, inlet gas temperature, and O3 concentration. Based on the physical nature of these variables and the frequency of their investigation, flow rate, temperature, and exhaust gas components are identified as the three main influencing variables. These variables are reviewed in detail below.

Table 1

Summary of the investigation on the correlation between system variables and morphology categories for exhaust gas recirculation coolers fouling

Reference	Year	System variable	Fouling morphology category
Ismail et al. [41]	2004	Cooler inlet header structure	Roughness
Abd-Elhady et al. [42]	2011	Flow rate	Thickness of fouling
Jang et al. [43]	2011	Cooler structures	Wetness
Malayeri et al. [44]	2013	Flow rate	Compactness; Size of particulate matter
Bravo et al. [45]	2013	Cooler structures	Wetness
Bravo et al. [46]	2013	Engine operation points	Compactness
Prabhakar and Boehman [28]	2013	Coolant temperature	Roughness
		Engine operation	Size and number of void

		condition	
Sluder et al. [47]	2014	Mass flow	Roughness
Kuhara et al. [48]	2014	Engine start mode	Roughness; Number of voids
Salvi et al. [49]	2014	Baking temperature	Roughness (Area ratio); Thickness of fouling
Arnal et al. [50]	2015	Fuel type	Orderliness of primary particle
Tanaka et al. [18]	2016	Wall temperature	Shape; Glossiness; Compactness
Hooman and Malayeri [51]	2016	Flow rate	Roughness
Matsudaira et al. [52]	2017	Cooler structures	Distribution state
Arnal et al. [53]	2018	Not reported	Orderliness of primary particle
Lance et al. [54]	2018	Soot concentration	Size of the primary particle; Porosity of primary particle
Paz et al. [37]	2019	Hydrocarbon concentration	Wetness; Glossiness
Paz et al. [29]	2021	Hydrocarbon concentration	Shape of primary particles; Roughness
Bera et al. [55]	2022	Heat temperature	Shape; Glossiness; Compactness
Li et al. [56]	2022	Hydrocarbon concentration	Size of dendritic structures; Thickness of fouling
Tomuro et al. [57]	2023	Coolant Temperature; Inlet gas Temperature	Compactness; Fragmentation
Vence et al. [40]	2023	Hydrocarbon concentration	Color; Wetness
Vence et al. [58]	2023	O_3 concentration	Color; Wetness

5.1. Effect of flow rate

The consequence of exhaust gas velocity or mass flow rate on fouling morphology is illustrated in **Figure 9**. Malayeri et al. compared fouling characteristics at two flow velocities, 10 m/s and 30 m/s, as shown in **Figure 9 (a)**. They observed that fouling formed at 10 m/s was more porous and had coarser particles [44]. Beyond conventional EGR coolers, Hooman and Malayeri examined the differences in fouling morphology for metal foam EGR coolers at 10 m/s and 30 m/s, as depicted in **Figure 9 (b)**. Their findings revealed that fouling at lower flow velocities was discontinuous and rough, whilst, at higher velocities, it was continuous and smooth [51]. Sluder et al.'s experimental results also confirmed that higher mass flow rates produce more uniform fouling [47]. Generally, higher gas velocities result in greater shear forces at the gas-fouling interface, leading to stronger fouling removal effects [12, 13, 19, 59]. Consequently, the morphological differences caused by flow velocity provide crucial evidence for understanding fouling removal mechanisms.

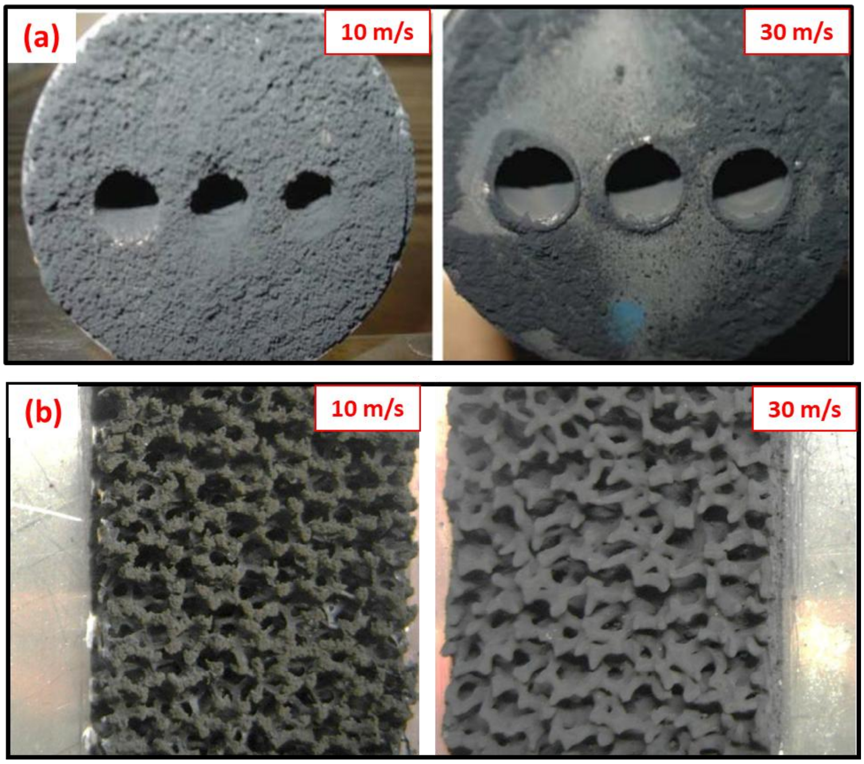

Figure 9. Effect of gas flow rate on fouling morphology. (a) Malayeri et al. [44], (b) Hooman and Malayeri [51].

5.2. Effect of temperature

Multiple studies have demonstrated that the cooler wall temperature significantly influences fouling morphology. As illustrated in **Figure 10**, Prabhakar and Boehman observed that fouling generated at 85 °C was rougher than that formed at 40 °C [28]. Tanaka et al. categorised fouling into distinct types based on formation temperature: 'soft deposit' at room temperature, 'low-temperature lacquer' at 80 °C, and 'high-temperature lacquer' at 100 °C, whilst no fouling occurred at 120 °C [18]. Although these two studies employed different morphological characterisation classifications, both indicated that variations in formation temperature affect fouling morphology. This consequence likely stems from temperature's strong influence on thermophoretic deposition and hydrocarbon condensation processes [12, 60, 61]. Therefore, the morphological differences caused by formation temperature provide valuable insights into understanding particulate matter deposition and condensation mechanisms.

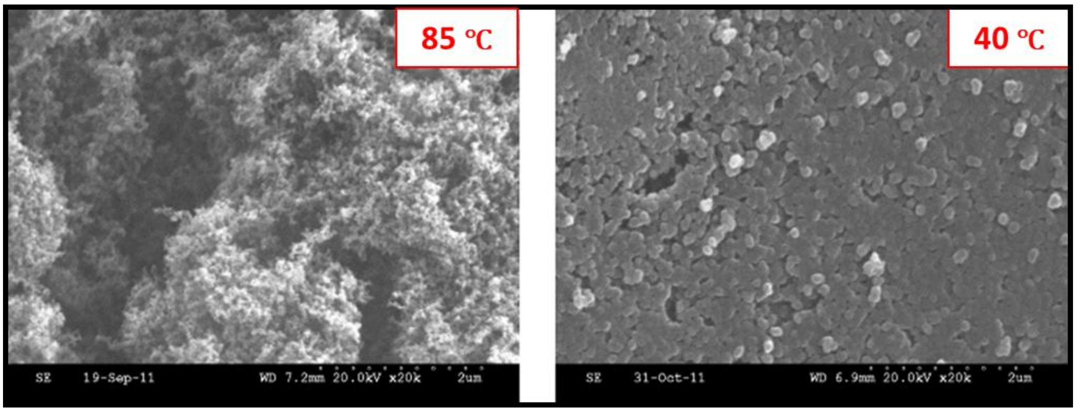

Figure 10. Effect of wall temperature on fouling morphology. From Prabhakar and Boehman [28]

5.3. Effect of exhaust gas components

Fouling consists of particulate matter deposition and vapour condensation from exhaust gases. Consequently, fouling morphology is significantly influenced by exhaust composition, which is directly governed by engine operating conditions. Based on this, researchers have compared the effect of engine load on fouling morphology. Prabhakar and Boehman compared fouling morphologies under two engine operating conditions (2150 rpm, 203 Nm and 1400 rpm, 81 Nm), as shown in **Figure 11**. They found that fouling under 203 Nm conditions had more numerous and finer pores, while fouling under 81 Nm conditions had larger but fewer pores [28]. Kuhara et al. compared fouling morphologies under cold start and hot start conditions. Results showed that fouling surfaces were smoother under cold start conditions, while hot start conditions produced fouling surfaces with more irregularities and pores [48].

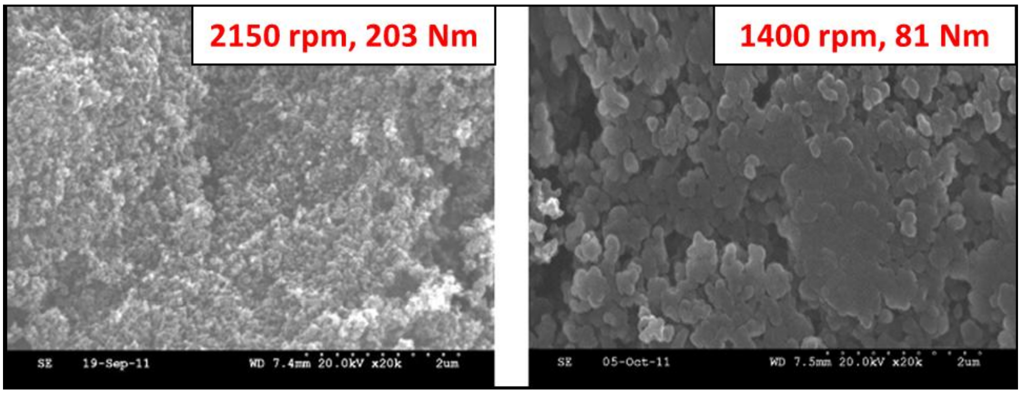

Figure 11. Effect of engine load on the fouling morphology [28]

Since changes in engine operating conditions involve simultaneous alterations of multiple key parameters (HC composition and concentration, soot concentration and size distribution, temperature, flow rate, etc.), it represents a composite external control variable. This approach makes it challenging to identify the influence of individual parameters on fouling morphology. Therefore, some researchers have adopted a single-variable approach to further investigate these issues. Lance et al. compared fouling morphologies under low and high soot concentration conditions, as shown in **Figure 12 (a)**. Results indicated that compared to low soot concentrations, high soot concentrations produced fouling with smaller primary particles and higher porosity [54]. Li et al. compared the influence of another key parameter - HC concentration on fouling morphology, as shown in **Figure 12 (b)**. They found that higher HC concentrations resulted in fewer but larger dendritic structures on the fouling surface due to enhanced particle agglomeration by the high concentrations of condensed hydrocarbons [56].

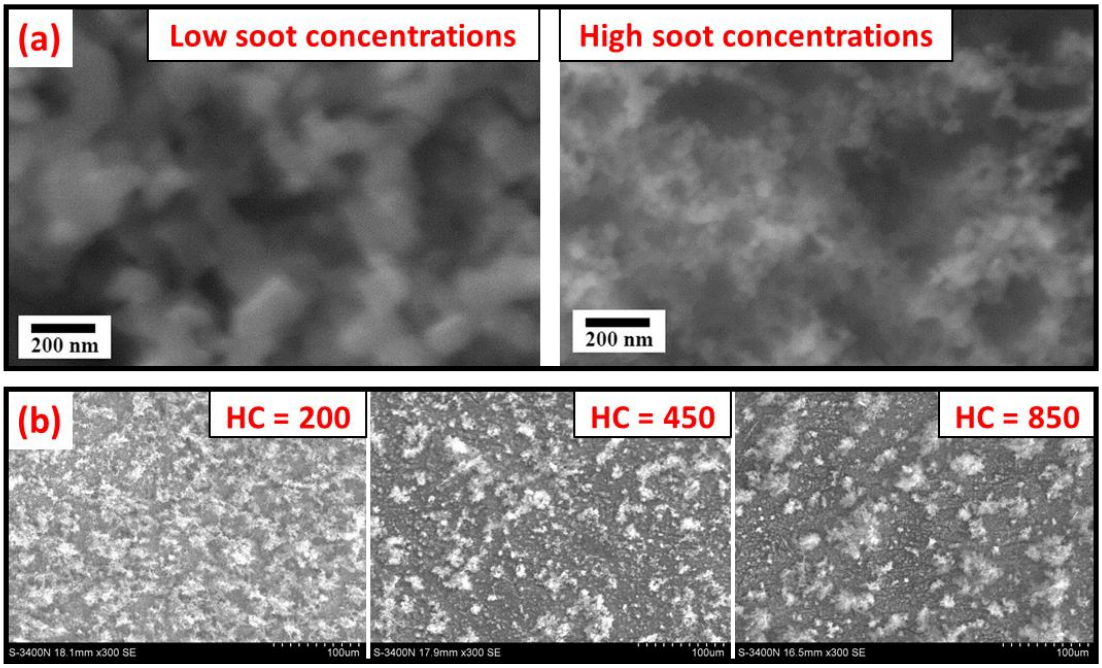

Figure 12. Effect of components of exhaust gas on the fouling morphology. (a) soot concentration [54], and (b) Hydrocarbon concentration [56]

This series of experiments exploring the correlation between exhaust composition and fouling morphology reveals the close relationship between fouling morphology and its constituent components. The results demonstrate that fouling morphology is highly correlated with the composition and proportion of particulate matter and hydrocarbons that constitute the fouling. Specifically, different compositions and proportions lead to different fouling morphologies. Furthermore, the introduction of condensed hydrocarbons further complicates this process, triggering more complex coupling effects. For instance, agglomeration effects caused by liquid-phase forces can make fouling structures more compact and smoother.

Therefore, studying the relationship between exhaust composition and fouling morphology not only helps understand fouling formation mechanisms but also provides new avenues for quantifying the contribution of each sub-component to fouling morphology.

In addition to the aforementioned system variables affecting fouling morphology, differences in cooler structures can also lead to the formation of different fouling morphologies [43, 52]. This is primarily due to changes in exhaust gas flow patterns caused by different structures, which simultaneously affect fouling deposition and removal mechanisms. Moreover, differences in fuel types can lead to changes in exhaust composition, thereby influencing fouling morphology [50].

This section discusses the influence of key variables on fouling morphology. Through the above analysis, we further recognise that multiple system variables jointly affect fouling morphology, as shown in **Figure 13**. This is because system variables are the original factors triggering fouling mechanisms. By controlling system variables, we can alter different types of mechanisms and their intensities, including but not limited to deposition mechanisms (such as particulate matter deposition and hydrocarbon deposition), removal mechanisms, and the relative contributions of various sub-mechanisms. Therefore, an in-depth study of the relationship between system variables and fouling morphology helps us to comprehensively understand complex fouling mechanisms.

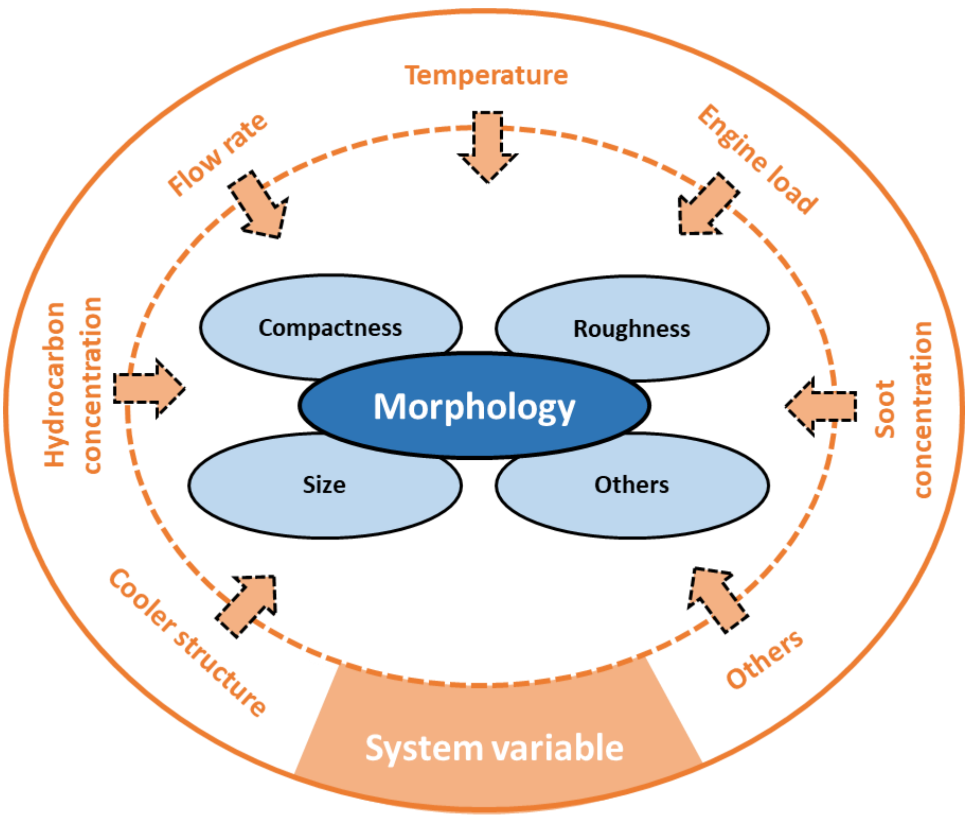

Figure 13. Overview of system variables affecting EGR coolers fouling morphology

6. The morphology–property correlation

Table 2 provides a concise summary of the 18 past studies that reported the relationship between fouling morphology and properties. The properties covered include density, thermal conductivity/thermal resistance, mechanical properties, water stability, crushing strength and stiffness, removal /shear stability, thermal stability, and adhesion force. Here, we categorise these into four groups: density, thermal properties, mechanical properties, and stability properties, which are elaborated upon in detail below.

Table 2

Summary of the investigation on the correlation between morphology and property for exhaust gas recirculation coolers fouling

Reference	Year	Fouling morphology category	Fouling property
Lance et al. [62]	2009	Porosity	Density; Thermal conductivity
Teng and Barnard [63]	2009	Size of pores; Porosity; Layering state	Thermal conductivity / thermal resistance; Mechanical properties
Teng and Barnard [64]	2010	Size of pores; Porosity; Layering state	Density; Thermal conductivity; Mechanical properties; Water stability
Lance et al. [65]	2010	Not reported	Water stability
Lance et al. [17]	2010	Connection way of particulate matters	Density
Lance et al. [66]	2011	Porosity/compactness	Density; Thermal conductivity; Crushing strength and stiffness
Abarham et al. [22]	2012	Fragmentation	Remove stability
Abarham et al. [23]	2013	Fragmentation	Remove stability
Furuhata et al. [30]	2014	Fragmentation	Remove stability
Salvi et al. [49]	2014	Compactness	Thermal stability
Han et al., [13]	2015	Fragmentation	Remove stability
Matsudaira et al. [52]	2017	Fragmentation	Remove stability
Lance et al. [54]	2018	Porosity	Density
Razmavar and	2019	Compactness	Adhesion force

Malayeri [67]			
Paz et al. [29]	2021	Porosity; Size of particulate matter; Wetness	Density
Cook et al. [55]	2022	Structure of pores	Thermal stability
Han et al. [39]	2023	Size and way of particulate matter connection	Thermal conductivity
Vence et al. [40]	2023	Wetness	Density

6.1. Density

The morphology of fouling is closely related to fundamental material properties such as density, colour, and phase state. Colour and phase state, being both morphological aspects and basic material properties, have been discussed previously and will not be elaborated upon here. This section focuses on the correlation between morphology and density.

Lance et al.'s research indicates that the average density of fouling is approximately 0.035 g/cm^3, with a porosity as high as 98% [62]. In a subsequent study, they further discovered that the low density is primarily due to the connection method between sub-units (particulate matters), which occurs through narrow bridges of only about 15 nm [17]. Vence et al.'s research found that fouling with more wet components also has a higher density [40]. Similarly, Lance et al. observed that hydrocarbon condensation encapsulating particulate matter can form fouling with fewer pores and greater density [54]. Paz et al. further quantified the density of fouling formed under different degrees of hydrocarbon condensation, providing a more comprehensive understanding of the relationship between condensation and fouling density [29]. Teng and Barnard proposed a three-layer substructure model for fouling, including a base layer, intermediate layer, and surface layer. The surface layer is highly porous with low density and thermal conductivity; the base layer has low porosity, high density, and the best thermal conductivity; the intermediate layer's pore morphology, density, and thermal conductivity are between the two [64].

Overall, morphological characteristics such as wetness, densification, and sub-unit connection methods are key factors influencing fouling density. This relationship between morphology and density not only enhances our understanding of fouling structure but also provides valuable insights for predicting and controlling fouling properties in practical applications.

6.2. Thermal property

Thermal conductivity is a core parameter of thermal properties. Lance et al. determined that the average thermal conductivity of fouling is approximately 0.041 W/(mK), significantly lower than that of metallic materials (e.g., 304 stainless steel at

14.7 W/(mK)) and closer to that of air (0.025 W/(mK)) and certain insulating materials (such as glass fibre and R-12 expanded and extruded polystyrene). This is primarily attributed to the high porosity of fouling [62]. A report by Lance et al. also indicated that thermal conductivity is mainly controlled by fouling density [66]. Teng and Barnard further developed a negative correlation curve between thermal conductivity and porosity based on literature and experimental results, demonstrating that higher porosity corresponds to lower thermal conductivity [64].

Teng and Barnard proposed a three-layer substructure model of fouling, suggesting that particle size and deposition patterns influence the morphology of the deposition layer. The thermal conductivity of the corresponding fouling layers decreases progressively (thermal resistance increases), from inner layers with micro pores (< 10 nm) to a randomly-packed intermediate layer with meso pores (10-50 nm), and finally to a loose surface layer with macro pores (> 50 nm) [63]. Han et al. posit that in scenarios involving hydrocarbon condensation, the enlargement of particulate matter within fouling may construct a more robust heat transfer framework, thereby enhancing overall thermal conductivity [39]. Generally, the morphological characteristics of fouling, particularly porosity and particle size, directly influence its thermal conductivity. Moreover, as thermal conductivity is closely related to density [64], morphological features affecting density also indirectly impact thermal conductivity.

6.3. Mechanical property

The relationship between the morphology and mechanical properties of the fouling may lie in their layered structure: the base layer, formed by nanoparticles through van der Waals forces and interactions with the metal surface, exhibits relatively high density; the intermediate layer has a moderate density; while the surface layer, composed of particle clusters connected by mechanical interlock, features high porosity and low density. This stratified structure highlights the intrinsic correlation between fouling morphology and mechanical properties [63, 64]. Lance et al. were the first to report the use of Load-Displacement Curves to characterise the crushing strength and stiffness of fouling, and they found that the load for Light-Duty fouling could approach approximately 1 kPa [66]. However, no results of Load-Displacement Curves for other types or forms of fouling were provided for comparison.

Razmavar and Malayeri discovered that fouling formed on treated coated surfaces was more porous than that on untreated surfaces, as evidenced by the surface adhesion of the two types of fouling. The results revealed that the adhesion of fouling to the substrate stainless steel was approximately three times greater than that to the coated surface, indicating that fouling on coated surfaces exhibits weaker adhesion and is consequently easier to remove [67]. This finding elucidates the close relationship between the compactness of fouling morphology and its adhesiveness. The results provide valuable insights for developing novel cleaning methods, potentially mitigating the adverse consequences of fouling.

6.4. Stability property

Research indicates a strong correlation between the thermal stability of fouling and its morphology. Cook et al. observed that raw fouling softens at 100°C and melts at 150°C, whereas an extracted soluble substance remained stable even at 300°C. They postulated that this enhanced thermal stability might result from the soluble substance obstructing the fouling's pores, thereby retarding oxidation [55]. Salvi et al. noted that fouling exhibited fragile dendritic features before high-temperature baking, but after one baking cycle, it displayed more agglomerated characteristics, with reduced area ratio, smoother surface, and decreased thickness. A second baking cycle further reduced the fouling thickness. They attributed this to the collapse of porous fouling structures due to higher kinetic energy during heating [49]. Thermal stability typically results from the combined effects of composition and morphology. Although quantitative studies distinguishing the specific contributions of morphology and composition to thermal stability are currently lacking, these findings clearly demonstrate the close relationship between fouling morphology and thermal stability. The porous structure of fouling influences its thermal stability, while thermal treatment alters the fouling morphology, creating a cycle of mutual influence.

Moreover, the morphology of fouling can change through hydration [64] or water immersion and drying [65]. These processes are complex but are generally related to the susceptibility of the porous fouling structure to collapse under liquid-phase forces and thermal stresses.

In addition to the aforementioned thermal and water stability, the evaluation of the remove/shear stability, which reflects the ease of removal of fouling by airflow shear forces, is also related to the morphology of the fouling. Han et al., in their conceptual model incorporating three removal mechanisms, pointed out that one scenario involves fouling being removed through airflow shear forces due to mud-cracking [13]. Furuhata et al. [30], Matsudaira et al. [52] and Abarham et al. [22, 23] observed how fouling was progressively removed in areas with a higher degree of fragmentation, as detailed in Section 4.1. Interestingly, experimental findings by Lance et al. reported that when fouling is stripped off, the fracture surface is within the fouling itself rather than at the fouling-metal interface, which may be associated with the presence of large voids within the layers [66]. Taken together, the degree of surface fragmentation and the presence of large voids within the fouling may be related to its stability against shear forces from exhaust airflow.

In conclusion, as shown in **Figure 14**, fouling morphology significantly affects its density, thermal, mechanical, and stability properties, which in turn directly determine cooler performance. For heat exchangers, the thermal conductivity of fouling is crucial and is primarily dependent on morphological characteristics such as porosity, wettability, and the scale of the heat transfer skeleton. Additionally, pressure drop, another critical parameter for evaluating heat exchanger performance, is mainly influenced by fouling thickness and surface topography. Fouling thickness results from the interplay between deposition and removal mechanisms, with removal effectiveness closely related to surface mechanical properties, which are influenced by fouling compactness. Despite the complex interrelationships between morphology and properties, in-depth analysis reveals that fouling morphology may be the more fundamental factor. It not only affects fouling thickness and surface topography but also further influences gas flow patterns, ultimately leading to negative consequences on pressure drop. Therefore, a deep understanding and control of fouling morphology are crucial for optimising heat exchanger performance.

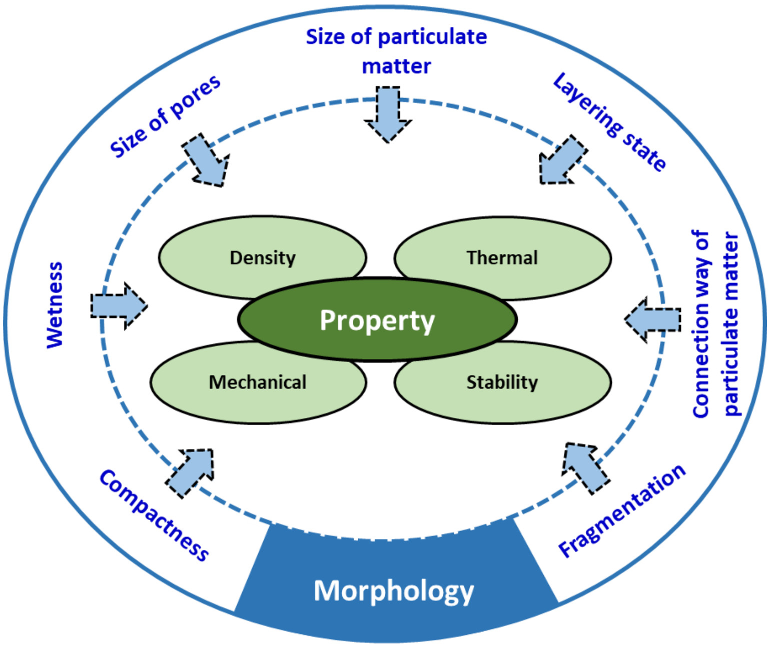

Figure 14. Overview of fouling morphology affecting fouling properties in EGR coolers

7. Challenges and opportunities

Throughout the review and analysis of EGR cooler fouling morphology, several limitations and challenges have been identified, which can serve as directions for future endeavours:

(1). Organic integration of multi-scale characterisation

Most studies typically focus on only one or two of the four scales (macro, meso, micro, and nano), with few encompassing all four. This limitation leads to an incomplete understanding of fouling morphology. However, a comprehensive and systematic understanding of the subject requires in-depth knowledge of each level, its sub-units, and their connections. Therefore, organic multi-scale or even full-scale morphological characterisation is a research direction worth exploring.

(2). Developing more quantitative morphological categories and indicators

Morphology covers three dimensions: shape, size, and structure, encompassing a series of characterisation categories, each of which can be realised through different characterisation indicators, resulting in considerable depth and rich hierarchical structure. However, based on the analysis of past literature, we found that morphological characterisation in most studies remains qualitative, with quantitative characterisation being relatively rare. This is evident in the literature, where textual descriptions predominate over precise data presentation. This *status quo* not only hinders the dissemination and horizontal comparison of scientific knowledge but also makes it difficult to clearly and directly convey characterisation results to peers or readers. Therefore, developing more quantitative morphological categories and indicators is of great significance. For instance, some fouling has been confirmed to have fractal characteristics [64, 68], yet verbal qualitative descriptions of them are often inadequate. Parameters from fractal science (such as fractal dimension, self-similarity dimension, etc.) could be employed for quantitative characterisation.

(3). Refining fouling nomenclature and taxonomy based on morphological science

Some disciplines have utilised morphology to complete the classification, naming, and mapping of research objects, which provides a common communication framework for the industry, such as [69-72]. However, in the EGR cooler fouling field, although mechanism-based classification and naming exist, this classification remains rudimentary. Morphology-based classification has only been addressed in a few studies and has not yet formed an industry consensus, remaining largely a blank field. Therefore, drawing on morphological classification experiences from other fields, establishing typical fouling morphologies, naming them, and creating atlases will be of significant value for standardisation in the fouling field.

(4). Refinement of fouling morphology evolution patterns over the full life cycle

Generation, growth, removal, stabilisation, and ageing are typically considered the complete lifecycle of fouling. Although previous studies have confirmed that morphology can provide intuitive visual evidence for the generation, growth, removal, and stabilisation processes of fouling, visual evidence for the ageing process is still lacking. Moreover, most studies focus on only one or two of these five classic stages, with varying time scales across different research projects, which may be short-term, medium-term, or limited to a specific stage. To date, no study has provided continuous evidence documenting the entire lifecycle evolution of fouling. Therefore, it is necessary to conduct in-depth research and enrich our understanding of the morphological evolution patterns of fouling throughout its entire lifecycle.

8. Conclusion

This comprehensive study on EGR cooler fouling morphology introduces a systematic overview that encompasses characterisation, spatiotemporal distribution nature, variable-morphology correlation, morphology-property correlation, and challenges and opportunities. The main findings and contributions are as follows:

(1). A characterisation framework for EGR cooler fouling morphology is developed, facilitating enhanced communication and comparative analysis among studies.

(2). Morphology plays a vital role in revealing the evolution process of fouling, including its generation and growth, and provides direct and explicit evidence for understanding fouling deposition and removal mechanisms. Meanwhile, it serves as a key perspective for understanding the intrinsic relationships between system variables, fouling, and properties.

(3). Future research on morphology could focus on the integration of multi-scale characterisation, the refinement of quantitative morphological categories and indicators, the development of nomenclature and taxonomy, and a comprehensive understanding of fouling evolution patterns.

This systematic review of EGR cooler fouling morphology deepens understanding of fouling generation and mitigation mechanisms and provides a crucial framework for advancing fouling morphology science.

Credit authorship contribution statement

Yipeng Yao: Conceptualization, Methodology, Writing – review & editing, Visualization, Supervision, Project administration. **Zhiqiang Han**: Conceptualization, Methodology, Validation, Investigation, Writing – review & editing. **Liping Luo**: Software, Formal analysis, Investigation, Visualisation. **Hai Du**: Writing – review & editing, Visualisation. **Wei Tian**: Formal analysis, Investigation, Visualisation. **Xueshun Wu**: Software, Writing – review & editing. **Zinong Zuo**: Writing – original draft. **Marie-Eve Duprez**: Writing – review & editing. **Guy De Weireld**: Writing – review & editing, Supervision.

Acknowledgements

The work is jointly funded by the National Defence Science and Technology Key Laboratory Fund Project [Grant Number: 2022-JCJQ-LB-062-0102] and the Sichuan Science and Technology Program [Grant Number 2023NSFSC0836]. Yipeng Yao acknowledges the joint scholarship of China Scholarship Council (CSC), Wallonie - Bruxelles International (WBI), and Belgian National Fund for Scientific Research (F.R.S.-FNRS) [Grant Number: 202208510023].

Data Availability

Data will be made available on request.

Declaration of generative AI and AI-assisted technologies in the writing process

During the preparation of this work, Yipeng YAO used ChatGPT to improve the readability and language of the manuscript. After using this service, the Yipeng YAO reviewed and edited the content as needed and take(s) full responsibility for the content of the published article.

Reference

[1] ZHAO Y, LI M, WANG Z, et al. Effects of exhaust gas recirculation on the functional groups and oxidation characteristics of diesel particulate matter [J]. Powder Technol, 2019, 346: 265-72.

[2] AL-QURASHI K, LUEKING A D, BOEHMAN A L. The deconvolution of the thermal, dilution, and chemical effects of exhaust gas recirculation (EGR) on the reactivity of engine and flame soot [J]. Combust Flame, 2011, 158(9): 1696-704.

[3] PAZ C, SUáREZ E, CONCHEIRO M, et al. Characterisation of the ozone effect on a scraped off fouling sample [J]. Powder Technol, 2024, 445: 120112.

[4] YAO Y, HAN Z, TIAN W, et al. Three condensation paths of exhaust and its five effects on exhaust gas recirculation (EGR) cooler fouling and thermal performance: A review [J]. Case Stud Therm Eng, 2023, 47: 103099.

[5] BOTT T R. Fouling of heat exchangers [M]. Elsevier, 1995.

[6] KHOSHNOOD A, MAEREFAT M, IMANI G, et al. Effect of soot particle deposition on porous fouling formation and thermal characteristics of an exhaust gas recirculation cooler [J]. Appl Therm Eng, 2023, 229: 120629.

[7] HOSEINI S S, NAJAFI G, GHOBADIAN B, et al. Experimental and numerical analysis of flow and heat transfer characteristics of EGR cooler in diesel engine [J]. Appl Therm Eng, 2018, 140: 745-58.

[8] BARATI H, WU M, KHARICHA A, et al. A transient model for nozzle clogging [J]. Powder Technol, 2018, 329: 181-98.

[9] BRAVO Y, ARNAL C, LARROSA C, et al. Impact on Fouling of Different Exhaust Gas Conditions with Low Coolant Temperature for a Range of EGR Cooler Technologies [J]. SAE Tech Pap, 2018, 2018-April.

[10] HOARD J, ABARHAM M, STYLES D, et al. Diesel EGR Cooler Fouling [J]. SAE Int J Engines, 2008, 1(1): 1234-50.

[11] ABD-ELHADY M S, MALAYERI M R, MüLLER-STEINHAGEN H. Fouling Problems in Exhaust Gas Recirculation Coolers In The Automotive Industry; proceedings of the International Conference on Heat Exchanger Fouling and Cleaning VIII - 2009, F, 2009 [C].

[12] ABARHAM M, HOARD J, ASSANIS D N, et al. Review of Soot Deposition and Removal Mechanisms in EGR Coolers [J]. SAE International Journal of Fuels and Lubricants, 2010, 3(1): 690-704.

[13] HAN T, BOOTH A C, SONG S, et al. Review and a conceptual model of exhaust gas recirculation cooler fouling deposition and removal mechanism; proceedings of the 11th Int Conf Heat Exch Fouling Clean, Engield (Dublin), Ireland, F Jun, 2015, 2015 [C]. Heat Exchanger Fouling and Cleaning.

[14] PAZ C, SUAREZ E, VENCE J, et al. Numerical Modelling of Fouling Process in EGR System: A Review [M]. Environmental Issues and Sustainable Development. 2021.

[15] SCHOENITZ M, GRUNDEMANN L, AUGUSTIN W, et al. Fouling in microstructured devices: a review [J]. Chem Commun (Camb), 2015, 51(39): 8213-28.

[16] LøGE I A, ANABARAONYE B U, FOSBøL P L. Growth mechanisms of composite fouling: The impact of substrates on detachment processes [J]. Chemical Engineering Journal, 2022, 446: 137008.

[17] LANCE M J, SLUDER C S, LEWIS S, et al. Characterisation of Field-Aged EGR Cooler Deposits [J]. SAE Int J Engines, 2010, 3(2): 126-36.
[18] TANAKA K, HIROKI K, KIKUCHI T, et al. Investigation of Mechanism for Formation of EGR Deposit by in situ ATR-FTIR Spectrometer and SEM [J]. SAE Int J Engines, 2016, 9(4): 2242-9.
[19] HAN T, SUL H, HOARD J, et al. The Effects of Temperature, Shear Stress, and Deposit Thickness on EGR Cooler Fouling Removal Mechanism - Part 1 [J]. SAE International Journal of Materials and Manufacturing, 2016, 9(2): 236-44.
[20] ISMAIL B, EWING D, CHANG J-S, et al. Development of a non-destructive neutron radiography technique to measure the three-dimensional soot deposition profiles in diesel engine exhaust systems [J]. J Aerosol Sci, 2004, 35(10): 1275-88.
[21] LANCE M J, BILHEUX H, BILHEUX J-C, et al. Neutron Tomography of Exhaust Gas Recirculation Cooler Deposits [J]. SAE Tech Pap, 2014, 1.
[22] ABARHAM M, CHAFEKAR T, HOARD J, et al. A Visualisation Test Setup for Investigation of Water-Deposit Interaction in a Surrogate Rectangular Cooler Exposed to Diesel Exhaust Flow [J]. SAE Tech Pap, 2012.
[23] ABARHAM M, CHAFEKAR T, HOARD J W, et al. In-situ visualisation of exhaust soot particle deposition and removal in channel flows [J]. Chem Eng Sci, 2013, 87: 359-70.
[24] SALVI A A, HOARD J, JAGARLAPUDI P K, et al. Optical and infrared in-situ measurements of EGR cooler fouling; proceedings of the SAE Tech Pap, F, 2013 [C].
[25] TANAKA K, SAKAI T, FUJINO T, et al. Evaluation of Mechanism for EGR Deposit Formation Based on Spatially- and Time-Resolved Scanning-Electron-Microscope Observation [J]. SAE Int J Adv Curr Pract Mobility, 2020, 3(1): 150-8.
[26] LI H, HOARD J, STYLES D, et al. Visual Study of In-Situ EGR Cooler Fouling Layer Evolution; proceedings of the Volume 1: Large Bore Engines; Fuels; Advanced Combustion; Emissions Control Systems, Columbus, Indiana, USA, F, 2014 [C]. American Society of Mechanical Engineers.
[27] SALVI A A, HOARD J, STYLES D, et al. In Situ Thermophysical Properties of an Evolving Carbon Nanoparticle Based Deposit Layer Utilising a Novel Infrared and Optical Methodology [J]. J Energy Res Technol, 2016, 138(5): 052207.1-.7.
[28] PRABHAKAR B, BOEHMAN A L. Effect of Engine Operating Conditions and Coolant Temperature on the Physical and Chemical Properties of Deposits From an Automotive Exhaust Gas Recirculation Cooler [J]. J Eng Gas Turbines Power, 2013, 135(2).
[29] PAZ C, SUáREZ E, VENCE J, et al. Evolution of EGR cooler deposits under hydrocarbon condensation: Analysis of local thickness, roughness, and fouling layer density [J]. Int J Therm Sci, 2021, 161.
[30] FURUHATA T, ABE Y, ZAMA Y, et al. Experimental study on PM deposition behavior in an EGR cooler [J]. Transactions of the JSME (in Japanese), 2014, 80(820): TEP0365-TEP.
[31] STYLES D, CURTIS E, RAMESH N, et al. Factors Impacting EGR Cooler Fouling - Main Effects and Interactions [Z]. 16th Directions in Engine-Efficiency and Emission Research Conference (DEER). Detroit, MI. 2010: 1-25
[32] LANCE M J, STOREY J, SLUDER C S, et al. Microstructural Analysis of Deposits on Heavy-Duty EGR Coolers [J]. SAE Tech Pap, 2013, 2.
[33] STOREY J M E, SLUDER C S, LANCE M J, et al. Exhaust Gas Recirculation Cooler Fouling in Diesel Applications: Fundamental Studies of Deposit Properties and Microstructure [J]. Heat Transfer Eng,

2013, 34(8-9): 655-64.

[34] YOO K H, HOARD J, BOEHMAN A, et al. Experimental Studies of EGR Cooler Fouling on a GDI Engine [J]. SAE Tech Pap, 2016, 2016-April.

[35] TIAN W, ZHANG X, ZHAO J. Particulate Deposit and Its Effect on Heat Transfer Efficiency for a Diesel Engine EGR Cooler [J]. Transactions of CSICE, 2017, 35(04): 326-31.

[36] AL-JANABI A, MALAYERI M R. Turbulence induced structures in Exhaust Gas Recirculation coolers to enhance thermal performance [J]. Int J Therm Sci, 2017, 112: 118-28.

[37] PAZ C, CONDE M, VENCE J, et al. Experimental study of the effect of hydrocarbon condensation on the fouling deposits of exhaust gas recirculation coolers; proceedings of the 13th Int Conf Heat Exch Fouling Clean, F Jun, 2019, 2019 [C].

[38] YUAN S, ZHAO C, CAI X, et al. Bubble evolution and transport in PEM water electrolysis: Mechanism, impact, and management [J]. Progress in Energy and Combustion Science, 2023, 96.

[39] HAN Z, YAO Y, TIAN W, et al. Effect of hydrocarbon condensation on fouling and heat exchange efficiency in EGR cooler [J]. Int J Therm Sci, 2023, 184: 12.

[40] VENCE J, PAZ C, SUáREZ E, et al. Analysis of the local growth and density evolution of soot deposits generated under hydrocarbon condensation: 3D simulation and detailed experimental validation [J]. Results Eng, 2023, 18: 101166.

[41] ISMAIL B, EWING D, COTTON J S, et al. Characterisation of the soot deposition profiles in diesel engine exhaust gas recirculation (EGR) cooling devices using a digital neutron radiography imaging technique [J]. SAE Tech Pap, 2004: 719-29.

[42] ABD-ELHADY M S, ZORNEK T, MALAYERI M R, et al. Influence of gas velocity on particulate fouling of exhaust gas recirculation coolers [J]. Int J Heat Mass Transfer, 2011, 54(4): 838-46.

[43] JANG S-H, HWANG S-J, PARK S-K, et al. Effects of PM fouling on the heat exchange effectiveness of wave fin type EGR cooler for diesel engine use [J]. Heat Mass Transfer, 2011, 48(6): 1081-7.

[44] MALAYERI M R, ZORNEK T, BALESTRINO S, et al. Deposition of Nanosized Soot Particles in Various EGR Coolers Under Thermophoretic and Isothermal Conditions [J]. Heat Transfer Eng, 2013, 34(8-9): 665-73.

[45] BRAVO Y, LARROSA C, ARNAL C, et al. Effects of soot deposition on EGR coolers: Dependency on heat exchanger technology and engine conditions; proceedings of the 10th Int Conf Heat Exch Fouling Clean, Budapest, Hungary, F Jun, 2013, 2013 [C].

[46] BRAVO Y, LUJAN J, TISEIRA A. Characterization of EGR Cooler Response for a Range of Engine Conditions [J]. SAE Int J Engines, 2013, 6(1): 587-95.

[47] SLUDER C S, STOREY J M, LANCE M J. Effectiveness stabilisation and plugging in EGR cooler fouling [J]. SAE Tech Pap, 2014.

[48] KUHARA K, SHIBASAKI Y, GOTO N, et al. Evaluation of Degradation Behavior of EGR-Cooler Performance and Deposits Characterization [J]. Transactions of Society of Automotive Engineers of Japan, 2014, 45(2).

[49] SALVI A, HOARD J, BIENIEK M, et al. Effect of Volatiles on Soot Based Deposit Layers [J]. J Eng Gas Turbines Power, 2014, 136(11).

[50] ARNAL C, BRAVO Y, LARROSA C, et al. Characterisation of Different Types of Diesel (EGR Cooler) Soot Samples [J]. SAE Int J Engines, 2015, 8(4): 1804-14.

[51] HOOMAN K, MALAYERI M R. Metal foams as gas coolers for exhaust gas recirculation systems

subjected to particulate fouling [J]. Energy Convers Manage, 2016, 117: 475-81.
[52] MATSUDAIRA N, IWASAKI M, HARA J, et al. Visualisation of the Heat Transfer Surface of EGR Cooler to Examine Soot Adhesion and Abruption Phenomena [J]. SAE Tech Pap, 2017.
[53] ARNAL C, BRAVO Y, LARROSA C, et al. Correlation between Real Diesel Fouled-EGRc Soot Samples and Soot Surrogates: Reactivity with NO and O2 and Chemical-Physical Characterization [J]. SAE Tech Pap, 2018.
[54] LANCE M J, MILLS Z G, SEYLAR J C, et al. The effect of engine operating conditions on exhaust gas recirculation cooler fouling [J]. Int J Heat Mass Transfer, 2018, 126: 509-20.
[55] BERA T, BROOM N, COOK S, et al. Thermogravimetric analysis applied to characterisation of the evolution of EGR deposits in a working engine [J]. Int J Engine Res, 2022, 24(5): 2113-25.
[56] LI J, ZHANG X, WU H, et al. Effect of Hydrocarbon Concentration on Particulate Deposition and Microstructure of the Deposit in Exhaust Gas Recirculation Cooler [J]. Int J Automot Technol, 2022, 23(3): 775-84.
[57] TOMURO M, BHADRA K, HEBERT J, et al. The Effect of Exhaust Emission Conditions and Coolant Temperature on the Composition of Exhaust Gas Recirculation Cooler Deposits [J]. SAE Tech Pap, 2023.
[58] VENCE J, PAZ C, SUAREZ E, et al. Experimental evaluation of the effect of ozone treatment on the oxidation and removal of dry soot deposits of the exhaust gas recirculation system [J]. Heliyon, 2023, 9(7): e17861.
[59] SLUDER C S, STOREY J, LANCE M J, et al. Removal of EGR Cooler Deposit Material by Flow-Induced Shear [J]. SAE Int J Engines, 2013, 6(2): 999-1008.
[60] HAN Z, LUO L, YAO Y, et al. Mapping of hydrocarbon condensation onset temperature and its sensitivity analysis for Exhaust Gas Recirculation (EGR) cooler [J]. Case Stud Therm Eng, 2024, 60: 104824.
[61] RAZMAVAR A R, MALAYERI M R. Thermal performance of a rectangular exhaust gas recirculation cooler subject to hydrocarbon and water vapor condensation [J]. Int J Therm Sci, 2019, 143: 1-13.
[62] LANCE M J, SLUDER C S, WANG H, et al. Direct Measurement of EGR Cooler Deposit Thermal Properties for Improved Understanding of Cooler Fouling [J]. SAE Tech Pap, 2009.
[63] TENG H, REGNER G. Particulate Fouling in EGR Coolers [J]. SAE Int J Commer Veh, 2009, 2(2): 154-63.
[64] TENG H, BARNARD M. Physicochemical characteristics of soot deposits in EGR coolers [J]. SAE Tech Pap, 2010.
[65] LANCE M J, SLUDER C S, BILHEUX H, et al. Characterisation of Field-Aged Exhaust Gas Recirculation Cooler Deposits [R], 2010.
[66] LANCE M J, SLUDER C S, BILHEUX H. Materials Issues Associated with EGR Systems [R], 2011.
[67] RAZMAVAR A R, MALAYERI M R. Mitigation of Soot Deposition on Modified Surfaces of Exhaust Gas Recirculation Coolers [J]. Heat Transfer Eng, 2019, 40(20): 1680-90.
[68] ABD-ELHADY M S, MALAYERI M R, MüLLER-STEINHAGEN H. Fouling Problems in Exhaust Gas Recirculation Coolers in the Automotive Industry [J]. Heat Transfer Eng, 2011, 32(3-4): 248-57.
[69] CARR J H. Clinical Hematology Atlas-E-Book: Clinical Hematology Atlas-E-Book [M]. Elsevier Health Sciences, 2021.
[70] VERRECCHIA E P, TROMBINO L. A visual atlas for soil micromorphologists [M]. Springer Nature,

2021.
[71] WYPYCH G. Material composition, structure and morphological features [J]. Atlas of Material Damage, 2017, 2: 7-57.
[72] MUKHERJEE S. Atlas of structural geology [M]. Elsevier, 2020.